

## H I LINE MEASUREMENTS OF EIGHT SOUTHERN PULSARS

BÄRBEL KORIBALSKI

Australia Telescope National Facility, CSIRO, P.O. Box 76, Epping, NSW 2121, Australia; bkoribal@atnf.csiro.au

SIMON JOHNSTON

Research Center for Theoretical Astrophysics, University of Sydney, NSW 2006, Australia; simonj@physics.su.oz.au

J. M. WEISBERG

Carleton College, Dept. of Physics and Astronomy, Northfield, MN 55057; jweisber@carleton.edu

AND

W. WILSON

Australia Telescope National Facility, CSIRO, P.O. Box 76, Epping, NSW 2121, Australia; wwilson@atnf.csiro.au

Received 1994 July 25; accepted 1994 September 22

### ABSTRACT

To derive their kinematic distances and to study the interstellar medium, we have measured 21 cm absorption and emission spectra in the direction of eight southern pulsars with the Parkes telescope. For the first time we have successfully obtained H I absorption measurements for PSRs J0908–4913, J1453–6413, J1456–6843, and J1709–4429. We have also significantly improved the sensitivity and resolution on PSRs J0742–2822, J1001–5507, and J1056–6258, whose spectra have previously been measured. Furthermore, we obtained a high-quality absorption spectrum on an eighth pulsar, PSR J1559–4438, whose previously determined spectrum was not usable for kinematic distance determinations due to frequency structure imposed by interstellar scintillation.

We present our absorption and emission spectra for these eight pulsars, derive kinematic distances and electron densities along their lines of sight where possible, and compare our results with previous work. For PSRs J1001–5507 and J1056–6258 we see H I in emission and absorption at velocities which cannot be explained by a simple rotation curve model. We present evidence to suggest that PSR J1056–6258 may be located behind the H II region BBW 328. We discuss the  $\gamma$ -ray efficiency of PSR J1709–4429 and its association with a supernova remnant in light of our kinematic distance estimate.

Additionally, we briefly examine the optical depths and the inferred spin temperatures of the interstellar gas clouds in the direction of some of the observed pulsars.

*Subject headings:* pulsars: general — radio lines: stars — stars: distances

### 1. INTRODUCTION

We obtained neutral hydrogen (H I) emission and absorption spectra in the direction of eight southern pulsars to obtain kinematic distance estimates and to study the cold gas phase of the interstellar medium (ISM). Here we present the spectra and distance estimates for the pulsars, four of which have not been observed before. Optical depths and inferred spin temperatures of the H I gas in the direction of these pulsars will be examined only briefly: a more detailed ISM study will be given in a subsequent paper.

The advantage of H I measurements against pulsars is their predictable pulsed nature, which allows us to study *both* absorption and emission along nearly the same line of sight (note that the absorption is seen only against the source whereas the emission is seen over the whole beam). Such observations together with a rotation curve or velocity field for the Galaxy allow the derivation of lower and/or upper distance limits, depending on the distribution of H I gas in the line of sight. There are several methods to derive pulsar distances, which we will now briefly discuss.

Distances to pulsars, as with most astronomical objects, are hard to obtain with a reasonable degree of precision. For pulsars, direct distance estimates can be obtained through parallax, by association with objects whose distances are known, and from kinematic measurements. Parallax distances are obtainable only for the closest pulsars ( $D < 1$  kpc), and

only four have been measured so far. Only a few pulsars have firm associations with globular clusters or supernova remnants and even then estimating the pulsar distances relies on knowing the distance of the associated object, which is also difficult to obtain. Thus the kinematic method remains as the method whereby most of the reliable pulsar distances have been obtained. The kinematic method can provide a lower limit to the pulsar distance when absorption is seen in an intervening H I cloud, and an upper limit in the absence of absorption at velocities with strong H I emission. To date,  $\sim 50$  pulsars have reliable upper and lower distance limits derived from their H I spectra (see the review of Frail & Weisberg 1990). Of these, only 14 have declinations below  $-10^\circ$ . The southern sources were done mostly in the mid-1970s (e.g., Ables & Manchester 1976), before the second Molonglo survey (Manchester et al. 1978) and the high-frequency Parkes survey (Johnston et al. 1992). These surveys discovered  $\sim 200$  pulsars between them, many of which are bright enough at 1400 MHz for H I measurements to be feasible. The development of the new 20 cm receiver at Parkes with a system temperature  $\sim 25$  K and a new 1024 channel digital correlator gave an added reason for observing a further sample of southern pulsars in H I.

Once distances have been obtained using any of the above methods, the electron density along the line of sight to the pulsar can be calculated from the pulsar's dispersion measure

(DM). With enough independent distance estimates throughout the Galaxy, a general Galactic electron density distribution can be created. The prevailing electron density model of the past 10 years (Lyne, Manchester, & Taylor 1985) has recently been replaced by the model of Taylor & Cordes (1993) due mostly to the increasing number of pulsars with measured H I distances. More measurements of kinematic distances are essential to improve further the model of the electron density. With the Taylor & Cordes model, the inverse procedure of obtaining a distance from the pulsar's DM can, in principle, be applied. But it should be stressed that distances obtained in such a manner can be in error by up to a factor of 2 along a given line of sight.

H I emission and absorption measurements toward pulsars not only lead to a model of the electron density in the Galactic disk, but also allow optical depth and temperature measurements of the neutral gas clouds in the interstellar medium.

Other ways to study the ISM in galaxies are H I and CO line emission observations which lead to the distribution and kinematics of the neutral atomic and molecular gas, respectively. H I absorption measurements against bright continuum sources in the Galactic plane are used to study the cold gas in front of them. H I emission and absorption measurements in nearly the same line of sight are most clearly made against pulsars and allow us to derive the optical depth and spin temperature (here roughly kinetic temperature) of the cold gas phase in front of the source. As the H I line emission comes from both cold and warm gas, we can in some cases also study the mixture of both gas phases.

2. OBSERVATIONS AND DATA ANALYSIS

H I observations toward eight southern pulsars were carried out on 1994 January 27–31 using the 64 m Parkes radio telescope. The new 20 cm system consists of a wideband (320 MHz) feed receiving two orthogonal linear polarizations and HEMT amplifiers with a noise figure of 12 K. The overall system temperature is 25 K on cold sky and the forward gain is 1.6 Jy K<sup>-1</sup>. The backend consists of a 1024 channel digital correlator, which was configured into two polarizations, each with 4 MHz of bandwidth. Velocity resolution in each polarization was then 7.8 kHz or 1.74 km s<sup>-1</sup>. Local oscillators, updated approximately once per hour, corrected for the changing Doppler shift of the observatory with respect to the local

TABLE 1  
OBSERVING PARAMETERS

PSR (J2000) (1)	INTEGRATION TIME		NUMBER OF PHASE BINS (4)	BIN WIDTH (ms) (5)
	Total (m) (2)	On-Pulse (m) (3)		
0742–2822.....	550	21	16	10.24
0908–4913.....	440	44	8	13.35
1001–5507.....	260	22	32	44.89
1056–6258.....	540	13	32	13.20
1453–6413.....	180	8	16	11.22
1456–6843.....	270	17	16	16.46
1559–4438.....	410	25	16	16.06
1709–4429.....	640	61	8	12.81

NOTES.—Col. (1), pulsar name (J2000); col. (2), total integration time; col. (3), on-pulse integration time; col. (4), number of bins in correlator configuration; and col. (5), bin width.

standard of rest (LSR). The pulsar period was divided into 8, 16, or 32 phase bins and spectral data were accumulated independently for each phase bin. (The number of bins was restricted by a minimum bin width of 10 ms.) Typical integration times were ~15 s and were always an integer multiple of pulse periods. By monitoring the pulse profile on-line, we adjusted the start time of the integration so that the pulse would be centered in one bin. This ensured maximum signal-to-noise ratios during the pulse. The pulsar parameters and the details of the observations are summarized in Tables 1 and 2.

The data were subsequently reduced off-line. A spectrum was formed for each pulsar phase bin and each polarization was then calibrated by the total power (i.e., the zero lag information). The “off” spectrum was then obtained by summing together the spectra from all the pulsar phase bins which did not contain the pulse. Similarly the “on” spectrum was obtained by summing spectra in the bins in which the pulse was present (usually only one, sometimes two, bins). The difference (i.e., on-off) spectrum is formed and normalized to the pulsar's intensity  $I_0$  for each polarization. A difference spectrum with reasonable signal-to-noise is obtainable in a ~30 minute integration. These difference spectra were then summed, after weighting by the square of the signal-to-noise ratio of the pulse profile.

TABLE 2  
OBSERVED PULSARS AND THEIR PARAMETERS<sup>a</sup>

PSR (J2000) (1)	$l$ (2)	$b$ (3)	DM (pc cm <sup>-3</sup> ) (4)	$D_{DM}$ (kpc) (5)	Period (ms) (6)	$S_{20}$ (mJy) (7)	PSR (B1950) (8)
0742–2822.....	243°77	-2°44	73.77	1.9	166.76	25.00	0740–28
0908–4913.....	270.27	-1.02	180.55	6.6	106.76	16.00	0906–49
1001–5507.....	280.23	+0.08	130.53	3.6	1436.59	8.00	0959–54
1056–6258.....	290.29	-2.97	320.80	14.0	422.45	24.00	1054–62
1453–6413.....	315.73	-4.43	71.07	1.8	179.48	16.00	1449–64
1456–6843.....	313.87	-8.54	8.65	$\pi$	263.38	80.00	1451–68
1559–4438.....	334.54	+6.37	58.80	1.6	257.06	40.00	1556–44
1709–4429.....	343.1	-2.7	75.69	1.8	102.45	9.00	1706–44

<sup>a</sup> From the catalog by Taylor, Manchester, & Lyne 1993.

NOTES.—Co. (1), pulsar name (J2000); col. (2), Galactic longitude,  $l$ ; col. (3), Galactic latitude,  $b$ ; col. (4), dispersion measure, DM. Where the dispersion measure differs from the values in the Taylor et al. pulsar catalog they have been taken from the GRO database of updated pulsar parameters held at Princeton. Col. (5), pulsar distance as derived from the dispersion measure and the electron density model by Taylor & Cordes 1993,  $D_{DM}$ ; col. (6), pulsar period; col. (7), 20 cm continuum flux density,  $S_{20}$ ; and col. (8), pulsar name (B1950).

The brightness temperature  $T_B$  of the emission spectrum was calibrated using the H I intensity contour plots derived by Kerr et al. (1986) at the longitude and latitude of the pulsar. We used a constant conversion factor for all spectra; the error in  $T_B$  is  $\sim 5$  K.

The intensity scale of the difference spectrum can also be expressed in units of  $\tau$ , the optical depth of the interstellar medium:  $I = I_0 \times e^{-\tau}$ . For a single, isothermal H I cloud we can then derive the spin temperature at a velocity,  $v$ , using the measured values for  $\tau$  and  $T_B$ :

$$T_{\text{spin}}(v) = \frac{T_B(v)}{1 - e^{-\tau(v)}}. \quad (1)$$

In practice, this simple situation is rarely encountered. When more than one cloud is present in the same line of sight and at a given velocity, or when the emission path length is longer than the absorbing path, the measured spin temperature is related in a complicated way to the true spin temperature (see, e.g., Kulkarni & Heiles 1988). In most of the Galactic H I disk collisions of hydrogen atoms with electrons and other particles determine the population of the two hyperfine levels, and  $T_{\text{spin}}$  closely approaches the kinetic temperature of the gas (see, e.g., Giovanelli & Haynes 1988).

### 3. RESULTS AND DISCUSSIONS

Figure 1 shows the emission and absorption spectra for each of the eight pulsars observed. Below the spectra we show the rotation curve derived for the longitude and latitude of the pulsar. In this paper we use an analytic expression given by the best-fit model of the Galactic rotation curve from Fich, Blitz, & Stark (1989). We adopt the standard IAU parameters (Kerr & Lynden-Bell 1986) for the distance to the Galactic center ( $R_0 = 8.5$  kpc) and the solar orbital velocity ( $V_0 = 220$  km s $^{-1}$ ). We define  $\omega_0$ , the angular rotation velocity at  $R_0$ , to be  $V_0/R_0 = 25.8824$  km s $^{-1}$  kpc $^{-1}$ . The radial velocity,  $V_r$ , for an object at a distance  $R$  from the Galactic center with a longitude  $l$  and latitude  $b$  is then

$$V_r = \left[ \omega(R) - \omega_0 + \frac{V_\pi \cos l}{R_0 \sin l} \right] R_0 \sin l \cos b, \quad (2)$$

where  $V_\pi = 4.2$  km s $^{-1}$  represents a net outward motion of the conventionally defined LSR with respect to Galactic objects and  $\omega(R)$  is the angular velocity given by the best-fit linear model of Fich et al. (1989):

$$\omega(R) = 1.00746 \times V_0/R - 0.017112 \times \omega_0. \quad (3)$$

Note that these equations indicate that gas at the solar circle has slightly nonzero velocity with respect to the conventionally defined LSR. The rotation curve of the Galaxy is the azimuthally smoothed average of its velocity field and thus implicitly assumes circular orbits around the Galactic center. It does not take into account the effects of streaming or random motions of the H I gas. Ideally, it would be best to use the observed velocity field to obtain the distances estimates. Recently, Brand & Blitz (1993) have completed a study of H II regions and reflection nebulae whose distances were known photometrically and whose radial velocities could be derived from their associated molecular clouds. This allowed them to derive the Galaxy velocity field over a longitude range of  $9^\circ < l < 270^\circ$ , out to a galactocentric radius of  $\sim 17$  kpc,

plus the region within 2–3 kpc from the Sun. Due to the small number of objects in their sample they smooth over a 1 kpc grid, and it should be noted that their data are rather sparse at distances greater than  $\sim 5$  kpc. In many regions, however, they find radial velocities in contradiction to the velocities derived from rotation curves. In the following discussion we will compare the velocities obtained from both methods where possible.

The lower and upper distance limits of pulsars can be inferred from their absorption and emission spectra, respectively. Following Frail & Weisberg (1990; § V.a) we set the lower distance limit,  $D_L$ , from the center of the farthest absorption feature in the spectrum and the upper distance limit,  $D_U$ , by the first emission peak above  $T_B = 35$  K and beyond the most distant absorption feature (see dotted lines in Fig. 1). The lower limit of 35 K on the brightness temperature is a conservative approach if one wishes to be certain of detecting absorption (Radhakrishnan et al. 1972; Weisberg, Boriakoff, & Rankin 1979). Weisberg et al. (1979), for example, found that sources lying behind H I with  $T_B > 35$  K rarely, if ever, display absorption with  $\tau < 0.3$ . Because, as described above, the simple Galactic rotation model cannot take into account the presence of random or streaming motions in the H I gas which causes departures from purely circular rotation, one must allow for errors of the order 7 km s $^{-1}$  when converting the observed velocities into distances (see, e.g., Weisberg et al. 1979; Shaver et al. 1982; Clifton et al. 1988). Table 3 shows the measured lower and upper velocity limits for each pulsar with the corresponding distance limits, where the distance errors are given by the 7 km s $^{-1}$  described above. We quote electron densities based on published dispersion measures and our best estimates of upper and/or lower distance limits. A discussion of the results for each pulsar is given below.

#### 3.1. PSR J0742–2822 (B0740–28); $l, b = 243^\circ 8, -2^\circ 44$

This pulsar was discovered at Bologna by Bonsignori-Facondi, Slater, & Sutton (1973) and soon observed in H I both by Gordon & Gordon (1973) and by Gomez-Gonzales et al. (1973). The latter had better signal-to-noise ratio in their spectra and derived a lower distance limit of 1.5 kpc based on an absorption feature of 6.8 km s $^{-1}$ . Their conservative estimate for an upper limit of 5.5 kpc was based on the absence of absorption at an emission feature near 70 km s $^{-1}$ ; they also

TABLE 3

H I KINEMATIC DISTANCES FOR PULSARS

PSR (J2000) (1)	$v_L$ (km s $^{-1}$ ) (2)	$v_U$ (km s $^{-1}$ ) (3)	$D_L$ (kpc) (4)	$D_U$ (kpc) (5)	$n_e$ (cm $^{-3}$ ) (6)
0742–2822...	+21.5	+69.3	2.0 $\pm$ 0.6	6.9 $\pm$ 0.8	0.011–0.037
0908–4913...	+9.9	+49.5	2.4 $\pm$ 1.6	6.7 $\pm$ 0.7	0.027–0.075
1001–5507...	–13.5	+34.7	...	6.9 $\pm$ 0.7	>0.011
1056–6258...	–18.2	–31.4	2.5 $\pm$ 0.5	2.9 $\pm$ 0.5	0.11–0.13
1453–6413...	–29.7	...	2.5 $\pm$ 0.5	...	<0.028
1559–4438...	–19.8	...	2.0 $\pm$ 0.5	...	<0.029
1709–4429...	–18.2	–29.7	2.4 $\pm$ 0.6	3.2 $\pm$ 0.4	0.024–0.032

NOTES.—Col. (1), pulsar name (J2000); cols. (2) and (3), lower and upper velocity limits,  $v_L$  and  $v_U$ , respectively, obtained from Fig. 1; cols. (4) and (5), adopted lower and upper distance limits,  $D_L$  and  $D_U$ , respectively, obtained from the Galactic rotation curve. In those cases where the rotation curve was not sufficient we also used the velocity field by Brand & Blitz (1993); col. (6), average electron density,  $n_e$ , along the line of sight derived from the distance limits and the pulsar dispersion measure.

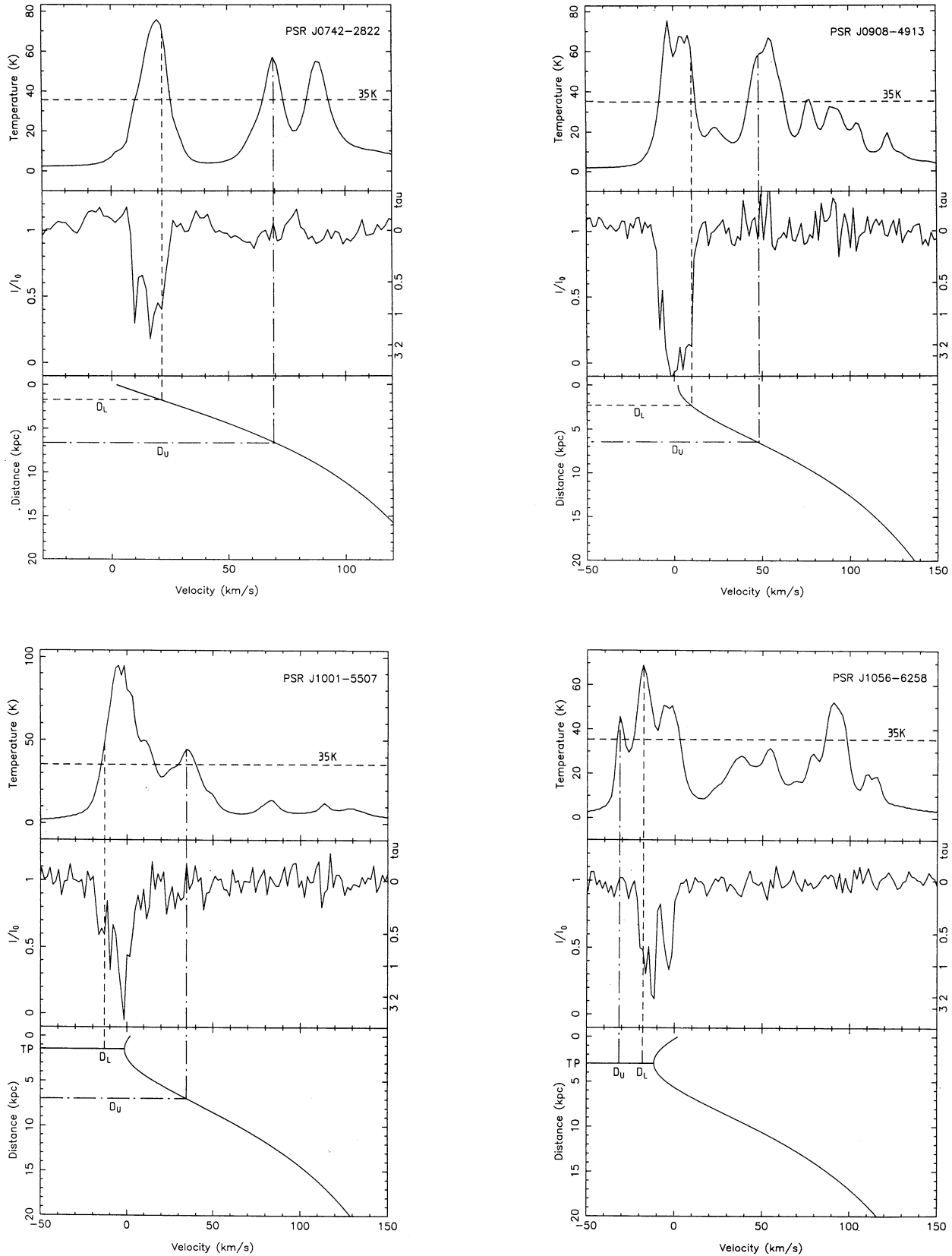


FIG. 1.—H I spectra in the direction of eight southern pulsars. The pulsar name (J2000) is given in the upper left or right corner of each plot. Each panel shows the H I emission spectrum on top, the weighted H I absorption spectrum in the middle, and the corresponding part of the Galaxy rotation curve on the bottom. Dotted lines indicate where the lower and upper distance limits were obtained. See the text for further description.

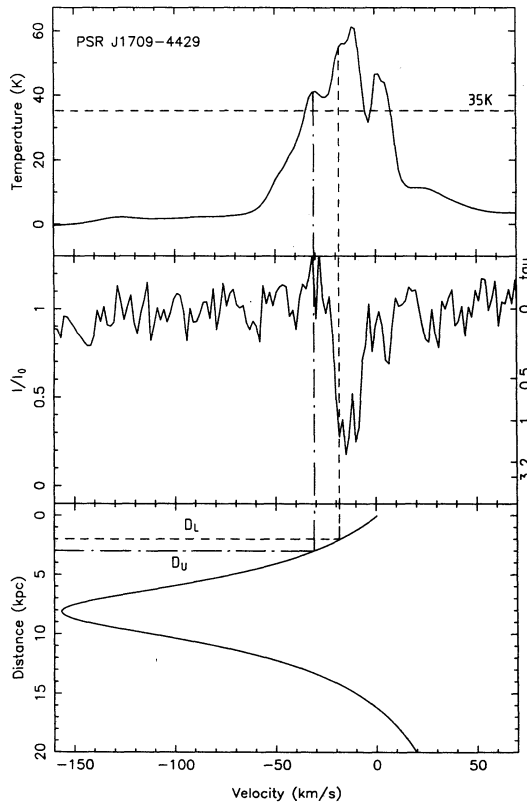
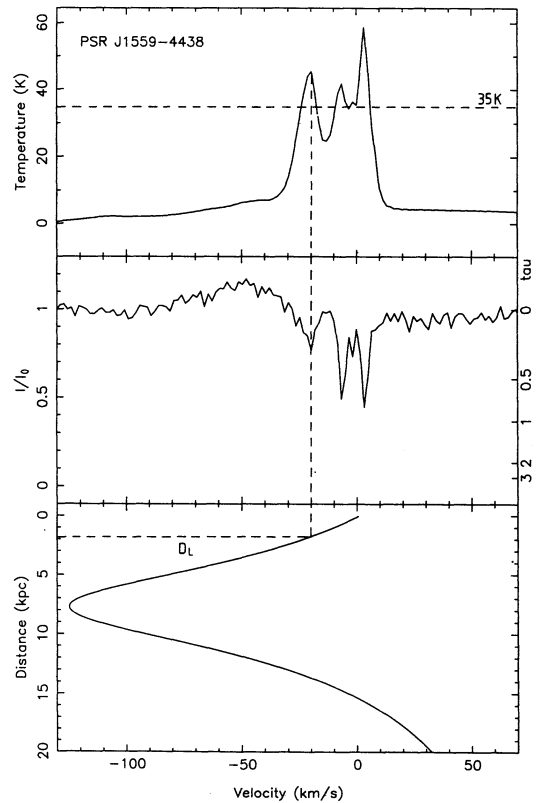
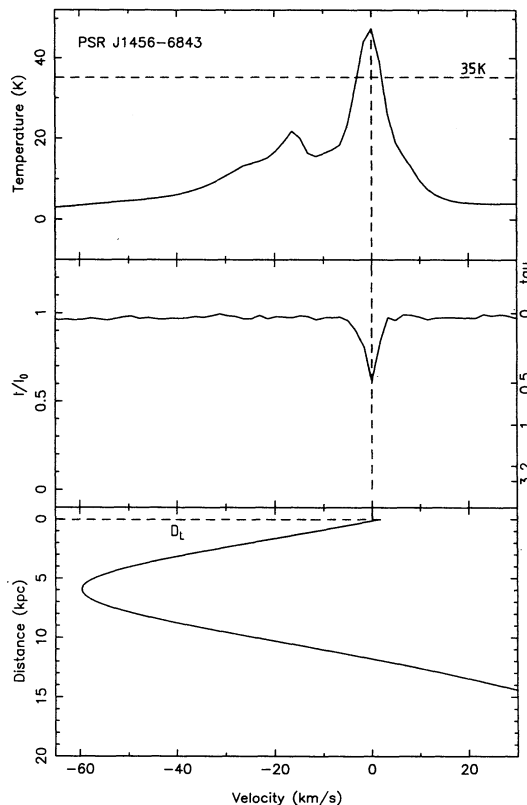
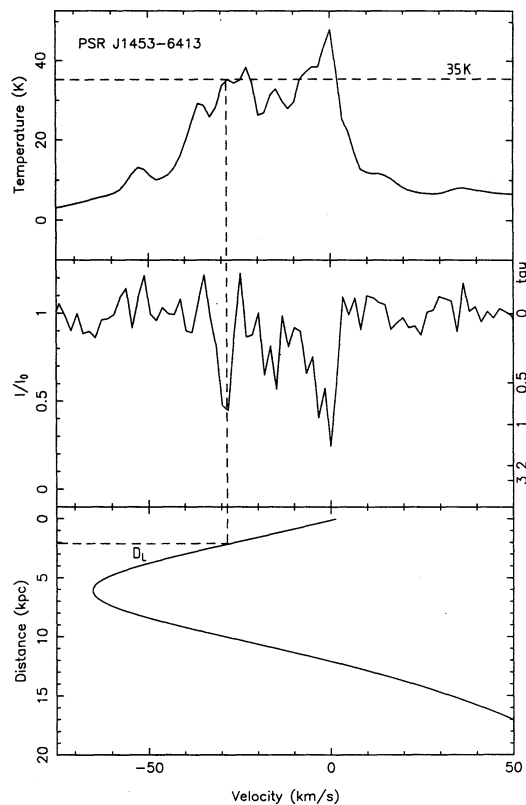


FIG. 1—Continued

claimed a less robust estimate of 2.5 kpc from an emission feature near  $32 \text{ km s}^{-1}$ . As Frail & Weisberg (1990) point out, this emission feature is too weak to expect any absorption. This is confirmed by our emission spectrum which shows very little H I emission and no absorption between 30 and  $60 \text{ km s}^{-1}$ . Frail & Weisberg give revised distances of  $D_L = 1.7 \pm 0.6 \text{ kpc}$  and  $D_U = 6.9 \pm 0.9 \text{ kpc}$ .

We find strong absorption at velocities between  $+7$  and  $+24 \text{ km s}^{-1}$ . The lower distance limit of  $D_L = 2.0 \pm 0.6 \text{ kpc}$  has been derived from the farthest absorption peak at  $+21.5 \text{ km s}^{-1}$ . No absorption has been found against the emission components around  $+69 \text{ km s}^{-1}$  and  $+87 \text{ km s}^{-1}$ , which sets the upper distance limit to  $D_U = 6.9 \pm 0.8 \text{ kpc}$ . The dip in the absorption feature at  $60 \text{ km s}^{-1}$  is almost certainly not real as it is within  $2\sigma$  of the noise. The values agree closely with those determined by Frail & Weisberg. They also agree well with the distances given by the observed velocity field of the Galaxy (Brand & Blitz 1993) in the direction of the pulsar.

The distance limits obtained can be used to place limits on the electron density along the line of sight, given knowledge of the pulsar's dispersion measure. The value of the Taylor & Cordes model along this line of sight is  $0.039 \text{ cm}^{-3}$  which is higher than our derived values of  $0.011\text{--}0.037 \text{ cm}^{-3}$ . Their model includes an explicit term for the Gum Nebula, whose outer regions lie along this line of sight (Taylor & Cordes 1993; Srinivasan Sahu & Sahu 1993). Our lower values of the electron density suggest that Taylor & Cordes may have overestimated the contribution of the Gum Nebula in this particular direction. Bailes et al. (1990b) measured a proper motion for this pulsar of  $(\dot{l}, \dot{b}) = (-9.8, -24.2) \text{ mas yr}^{-1}$ . This yields a transverse velocity range between  $250 \text{ km s}^{-1}$  and  $860 \text{ km s}^{-1}$  from our upper and lower distance limits.

Stacy & Jackson (1982) report an expanding H I shell at velocities ranging up to  $20 \text{ km s}^{-1}$ , which they argue is associated with the pulsar. While the pulsar's lower kinematic distance limit is similar to Stacy & Jackson's kinematic distance estimate for the shell the wide range of possible pulsar distances and the proper motion vector directed along the shell rather than from its center indicates that the proposed association is at best tentative only.

The highest optical depth of  $\tau \sim 1.5$  is found at  $v = 18 \text{ km s}^{-1}$ , implying a spin temperature of  $\sim 90 \text{ K}$  assuming a simple, single-cloud model.

### 3.2. PSR J0908–4913 (B0906–49); $l, b = 270^\circ 27', -1^\circ 02'$

This pulsar was discovered in the third Molonglo survey (D'Amico et al. 1988) and has not previously been observed in H I. We have detected H I absorption in the velocity range from  $-12$  to  $+14 \text{ km s}^{-1}$ . None of the other emission features ( $+24 \text{ km s}^{-1}$  to at least  $+120 \text{ km s}^{-1}$ ) shows absorption, though the closest emission feature at  $24 \text{ km s}^{-1}$  is quite weak ( $\sim 20 \text{ K}$ ). We definitely can place the pulsar closer than the emission component at  $50 \text{ km s}^{-1}$ , which shows no absorption. Caswell et al. (1975) found strong H I absorption in the  $50 \text{ km s}^{-1}$  emission feature in RCW 42 (G274.0–1.1), providing further support for our upper distance limit at that emission feature. We derive a lower distance limit of  $D_L = 2.4 \pm 1.6 \text{ kpc}$  from the absorption peak at  $10 \text{ km s}^{-1}$  and an upper distance limit of  $6.7 \pm 0.7 \text{ kpc}$  from the emission feature at  $50 \text{ km s}^{-1}$ . The lower limit agrees reasonably well with the observed Galaxy velocity field of Brand & Blitz (1993). Their data include a nebula with a velocity of  $9.8 \text{ km s}^{-1}$  at a distance of  $3.4 \pm 0.7 \text{ kpc}$ , in good agreement with our lower limit. Their

smoothed velocity contours indicate a distance of larger than  $10 \text{ kpc}$  for a velocity of  $50 \text{ km s}^{-1}$  but, due to a scarcity of nebulae at distances larger than  $5 \text{ kpc}$ , we prefer to use the distance limit derived from the standard rotation curve.

The electron density limits from these observations are  $0.027\text{--}0.075 \text{ cm}^{-3}$  which can be compared to the value of  $0.027 \text{ cm}^{-3}$  derived by the Taylor & Cordes model along this line of sight which probes to within  $\sim 10^\circ$  of the center of the Gum Nebula.

The optical depth is very high ( $\tau \gtrsim 2$ ) for most of the absorption features and indicates spin temperatures as low as  $70 \text{ K}$  in the direction of PSR J0908–4913.

### 3.3. PSR J1001–5507 (B0959–54); $l, b = 280^\circ 23', +0^\circ 08'$

PSR J1001–5507 was discovered in the first Molonglo survey by Wielebinski, Vaughan, & Large (1989). H I absorption measurements were carried out by Manchester, Wellington, & McCulloch (1981) using the Parkes telescope. They found absorption from about zero velocity to the tangential point at negative velocities and therefore only derived an upper limit for the distance of  $D_U = 6 \text{ kpc}$ , which Frail & Weisberg revised to  $D_U = 7.1 \pm 0.7 \text{ kpc}$ . We derive a similar upper distance limit,  $D_U = 6.9 \pm 0.7 \text{ kpc}$ , from an absence of absorption against the feature at  $34.7 \text{ km s}^{-1}$  in our spectrum. There is a rather strong ( $\sim 50 \text{ K}$ ) feature at  $11.5 \text{ km s}^{-1}$  at which we would expect to see absorption if the pulsar were located beyond this cloud. In fact, there is a slight dip in the absorption spectrum, but it is only  $\sim 2\sigma$  from the noise level and not very pronounced. Thus, although we keep  $6.9 \text{ kpc}$  as our robust upper distance limit we note that it could be as low as  $4.3 \text{ kpc}$ .

Absorption is observed at all negative velocities also having emission. Similar behavior is seen in the absorption spectrum of G282.0–1.2 and RCW 49 (G284.3–0.3) (Goss et al. 1972). Note that these relatively large negative velocities are not allowed in the Fich et al. (1989) model. They result from streaming motions in the Carina Arm of the Galaxy. The data of Brand & Blitz (1993) are too sparse in the direction of this pulsar to arrive at any firm conclusions regarding the distance of this streaming gas. Other investigators have found strong disturbances in the velocity field at this longitude, where we are looking right along the tangent to the Carina Arm. Hence we cannot determine a lower distance limit. Taylor & Cordes (1993) and Srinivasan Sahu & Sahu (1993) indicate that this line of sight does not intersect the bulk of the Gum Nebula.

The highest optical depth ( $\tau = 2\text{--}3$ ) for the absorption feature at about  $-2 \text{ km s}^{-1}$  indicates a spin temperature of  $\sim 100\text{--}110 \text{ K}$ .

### 3.4. PSR J1056–6258 (B1054–62); $l, b = 290^\circ 29', -2^\circ 9'$

This pulsar was discovered in the second Molonglo survey (Manchester et al. 1978) and a low-resolution H I spectrum was obtained by Manchester et al. (1981). They derived the distance limit to be near the tangent point, but they also noted absorption features at both  $50$  and  $100 \text{ km s}^{-1}$  which, if real, would imply a distance greater than  $15 \text{ kpc}$ . An unpublished spectrum by Manchester (private communication) showed no absorption feature at  $50 \text{ km s}^{-1}$ , but appeared to support the higher velocity absorption feature. Based on this, Frail & Weisberg thus determined a lower distance limit of  $16.1 \text{ kpc}$ . We reobserved this pulsar with higher velocity resolution and better sensitivity in an effort to clarify earlier results. We find no absorption at any positive velocity components; the rms of the optical depth is  $\sim 0.07$  in this region.

Interestingly we find both emission and absorption features at large negative velocities which cannot be fitted with the Galactic rotation model we are using. In particular, the lack of absorption against the strong feature at  $-32 \text{ km s}^{-1}$ , coupled with the presence of absorption at  $-18 \text{ km s}^{-1}$ , shows that the pulsar must lie between them. The velocity field is somewhat better behaved in this direction, and Brand & Blitz (1993) list several H II regions in the vicinity with radial velocities of approximately  $-20 \text{ km s}^{-1}$  and distances of  $\sim 2.5 \text{ kpc}$ . We take this to be our lower distance limit,  $2.5 \pm 0.5 \text{ kpc}$ . Brand & Blitz do not have any H II regions with velocities as negative as  $-30 \text{ km s}^{-1}$  until  $l = 296^\circ$ , where there are three at distances of 3–4 kpc, indicating that the pulsar is closer than these H II regions. Goss et al. (1972) observed H I absorption against several sources in this direction. These sources, G285.3–0.0, Eta Carina Nebula (G287.4–0.6), G290.1–0.8, NGC 3576 (G291.3–0.7) and NGC 3603 (G291.6–0.5) show absorption at all negative velocities where emission is present, even those velocities forbidden by the Fich et al. model. Several of them show particularly strong absorption in the range  $-20$  to  $-30 \text{ km s}^{-1}$ , even though these velocities are at the skirts of the H I emission. Unfortunately, none of these spectra show our emission feature at  $-30 \text{ km s}^{-1}$  which must be beyond the pulsar, so they are not useful in estimating its distance.

The Kerr et al. (1986) H I emission survey shows that the most negative velocity emission occurs near the latitude of this pulsar ( $b \sim -3^\circ$ ) over much of the longitude range of  $280^\circ$ – $295^\circ$ . The pervasive nature of this emission indicates that it is associated with large-scale Galactic structure. Optical (Graham 1970; Alfaro, Cabrera-Cano, & Delgado 1992) and CO (Grabelsky et al. 1987) studies of the Carina Arm show that it is also displaced to the south, with the CO study showing emission at negative velocities with this same longitude range that is attributed to orderly motions in the Carina Arm. Therefore it appears likely that the most negative velocity H I emission is generated in the Carina Arm near the tangent point. Consequently, we place our upper distance limit at the tangent point distance of 2.9 kpc. These distance limits imply a high electron density along this line of sight, between  $0.11$  and  $0.13 \text{ cm}^{-3}$  which is a factor of 2–3 times higher than expected in this outer Galaxy region.

It should be noted that one of the nebulae in this direction, BBW 328, a reflection nebula in the catalog of Brand, Blitz, & Wouterloot (1986) lies very close to the pulsar on the sky. It has a velocity of  $-12 \text{ km s}^{-1}$  and a distance of 3.1 kpc. This reflection nebula is part of one of the Carina OB associations (van den Bergh & Herbst 1975; Herbst 1975) and it is interesting to speculate that the pulsar might also originate from the stars in this complex. If we assume that the pulsar is located behind, or in, this nebula, then the nebula would contribute significantly to the dispersion measure. According to the Taylor & Cordes (1993) model, a distance of 3.5 kpc in this direction corresponds to a dispersion measure of  $140 \text{ cm}^{-3} \text{ pc}$ . The extra contribution of  $180 \text{ cm}^{-3} \text{ pc}$  from this nebula is not unreasonable for their typical electron densities of  $\sim 100 \text{ cm}^{-3}$ . This pulsar has also a moderately high scattering time of 23 ms at 408 MHz (Alurkar, Slee, & Bobra 1986). This combination of unusually high dispersion measure and scattering time has been noticed in two other pulsars, PSRs B1849+00 and B1758–23 (Frail & Clifton 1989; Frail, Kulkarni, & Vashisht 1993), both of which have foreground supernova remnants along the line of sight. This same effect, on a smaller scale, is likely to be happening with PSR J1056–6258 and the H II region BBW 328.

Humphreys & Kerr (1974) have made an extensive study of unusual motion in stars and gas in the  $(l, b) = (290, 0)$  region. Unfortunately, it appears that the gas in the direction of the pulsar is kinematically distinct from the gas in their study. Cowie et al. (1981) also studied an expanding supershell surrounding the Carina OB1 and OB2 associations at  $(l, b) = (289, 0)$  which may intersect the line of sight.

The optical depth of most of the observed absorption features lies between  $\tau = 1$ – $2$  and indicates spin temperatures of 60–110 K.

### 3.5. PSR J1453–6413 (B1449–64); $l, b = 315^\circ 73', -4^\circ 43'$

This pulsar was discovered at Molonglo by Large, Vaughan, & Wielebinski (1969). Ables & Manchester (1976) observed PSR J1453–6413 in H I but their spectrum was too noisy to derive useful kinematic distances. We find the farthest absorption feature centered at  $-29.7 \text{ km s}^{-1}$ , leading to a lower limit of  $2.5 \pm 0.5 \text{ kpc}$ . No upper distance limit can be derived due to an absence of strong H I emission at greater distances along this line of sight. Our lower limit of 2.5 kpc puts an upper limit of  $0.028 \text{ cm}^{-3}$  on the electron density along this line of sight and this is already substantially lower than the value of  $0.039 \text{ cm}^{-3}$  expected from the Taylor & Cordes (1993) model. The lower distance limit implies a transverse velocity for the pulsar of at least  $270 \text{ km s}^{-1}$  as derived from the proper motion measurements by Bailes et al. (1990b).

The optical depth is  $\sim 0.7$ – $0.8$  in the prominent absorption features and leads to spin temperatures of  $\sim 70 \text{ K}$ .

### 3.6. PSR J1456–6843 (B1451–68); $l, b = 313^\circ 87', -8^\circ 54'$

PSR J1456–6843 was also discovered at Molonglo by Large, Vaughan, & Wielebinski (1968). This pulsar has a small dispersion measure, and its distance obtained from parallax measurements by Bailes et al. (1990a) is  $450 \pm 60 \text{ pc}$ . As expected for a high-latitude pulsar, the emission spectrum shows only local H I and an absence of gas at large distances. The absorption spectrum shows moderate absorption against the local gas and does not allow a determination of a kinematic distance.

### 3.7. PSR J1559–4438 (B1556–44); $l, b = 334^\circ 54', +6^\circ 37'$

This pulsar was discovered at Molonglo by Vaughan, Large, & Wielebinski (1969). A high-resolution H I spectrum was obtained by Frail et al. (1991) showing several absorption components, but their baseline was strongly affected by interstellar scintillation. They identify absorption at two velocities,  $+2$  and  $-9 \text{ km s}^{-1}$ , which they concluded were most likely local absorption features, and therefore no kinematic distance was assigned. As can be seen from our absorption spectra, we were also affected by strong scintillations of the pulsar and, somewhat surprisingly, our spectrum shows “negative absorption” at similar velocities to the Frail et al. (1991) spectrum. Nevertheless we are confident that the absorption against the emission at a velocity of  $-19.8 \text{ km s}^{-1}$  is real, and this provides a lower distance limit of  $2.0 \pm 0.6 \text{ kpc}$ . The lack of strong emission at large distances once again precludes determining an upper limit. In this case, the Taylor & Cordes model is in reasonable agreement with our upper limit on the electron density of  $0.029 \text{ cm}^{-3}$ .

The optical depth of  $\tau \sim 0.2$ – $0.5$  implies a spin temperature between 100 and 220 K, again significantly higher than the temperatures derived for the other directions toward pulsars at lower latitude.

3.8. PSR J1709–4429 (B1709–44);  $l, b = 343^\circ.1, -2^\circ.7$ 

For PSR J1709–4429, a good kinematic distance can be obtained since there are two strong components in the emission spectrum close to each other, one seen in absorption and the other not. The farthest HI absorption feature peaks at  $-18.2 \text{ km s}^{-1}$  indicating a  $D_L$  of  $2.4 \pm 0.6 \text{ kpc}$ , whereas the emission is visible until  $-29.7 \text{ km s}^{-1}$ , indicating an upper limit of  $3.2 \pm 0.4 \text{ kpc}$ . These distance limits set limits on the electron density between  $0.024$  and  $0.032 \text{ cm}^{-3}$ . This is close to the “canonical” value of  $0.03 \text{ cm}^{-3}$  but is lower than the density derived from the Taylor & Cordes model in this region of the Galaxy.

PSR J1709–4429 was discovered in a high-frequency survey of the southern Galactic plane (Johnston et al. 1992). It has a short period and a characteristic age of only 17,000 yr. It is one of only a small handful of isolated radio pulsars to have been detected at high energies. Following the radio discovery it was detected in the X-ray band using *ROSAT* by Becker, Predehl, & Trümper (1992) and later detected in  $\gamma$ -rays with the EGRET instrument aboard *GRO* by Thompson et al. (1992) and at TeV energies by Kifune et al. (1993). The conversion of the spin-down energy to  $\gamma$ -ray flux was derived as  $\sim 2\%$  by Thompson et al. assuming a distance of 1.5 kpc. If we assume the same beaming fraction as Thompson et al. and the new kinematic distance of between 2.4 and 3.2 kpc then the efficiency goes up to between 4.6% and 8.2%. This revision, however, still implies that the pulsar’s efficiency is less than that of Geminga and substantially less than that of PSR B1055–52 (Fierro et al. 1993). This means that the general trend in the six known  $\gamma$ -ray pulsars of increasing efficiency with age as noted by Fierro et al. still holds, although this may be due to a selection effect. Information on the X-ray spectrum of this pulsar is sketchy (Becker et al. 1992) but from the details given, the lower limit to the X-ray efficiency is  $\sim 10^{-4}$ .

This pulsar has also been associated with a supernova remnant (McAdam, Osborne, & Parkinson 1993) based on the presence of a low-brightness partial shell coincident on the sky with the pulsar. Although the distance to the remnant is unknown, they argued that a small, bright infrared ridge is associated with the remnant and that the ridge was bright enough to have been seen with the Durham-Parkes HI emission survey (Strong et al. 1982). This has a localized feature at  $-32 \text{ km s}^{-1}$ , which leads to a distance of 3 kpc. They took this distance to be the distance of both the remnant and the pulsar. This turned out to be somewhat fortuitous, as in our pulsar observation there is strong emission at  $-32 \text{ km s}^{-1}$  but no trace of absorption. Thus, we believe that the ridge is located behind the pulsar and possibly not associated with the

remnant either. Even so, our distance limits still encompass the 3 kpc assumed by McAdam et al. (1993).

If we assume that the remnant and the pulsar are associated, and we place both at  $\sim 2.7 \text{ kpc}$ , then the diameter of the remnant is 30 pc and the pulsar is  $\sim 14 \text{ pc}$  from the center of the remnant. This leads to a velocity of  $\sim 800 \text{ km s}^{-1}$  for the pulsar to travel 14 pc over 17,000 yr. This is high compared to most pulsars with measured proper motions, but not unusually high for the postulated underlying pulsar distribution (Lyne & Lorimer 1994). However, the derived distance to the supernova remnant makes its age problematical. Using the relation of Caswell & Lerche (1979), the age of the remnant is less than 5000 yr. This is lower than the pulsar’s age by a factor of  $\sim 4$  and a low-energy explosion into a high-density medium would then have to be invoked in order to increase the remnant’s age. Recently, Frail, Goss, & Whiteoak (1994) have cast some doubt on the association with the shell remnant. Instead, their VLA image of the region shows a faint plerion which may be associated with the pulsar. Postulating an association with the plerion removes the problem of both the velocity of the pulsar and the age of the shell, but this association must still be regarded as tentative.

The optical depth of the observed absorption features is about one and indicates a spin temperature of  $\sim 90 \text{ K}$ .

## 4. CONCLUSIONS

We have measured HI absorption and emission spectra in the direction of eight southern pulsars with the Parkes telescope. Using an analytic expression for the Galactic rotation curve derived by Fich et al. (1989) and in some cases the Galactic velocity field by Brand & Blitz (1993) or Kerr et al. (1986), we have derived kinematic distances for all but one pulsar, PSR J1456–6843, whose distance is known from parallax measurements (Bailes et al. 1990a). For four pulsars we were able to give lower and upper distance limits; only one limit could be obtained for the other three pulsars. We also quote the electron densities in the direction of each pulsar as obtained from its kinematic distance and dispersion measure. Optical depths and spin temperatures of the interstellar clouds in the line of sight to the observed pulsar are only briefly mentioned; a detailed study will follow in a subsequent paper.

We thank the Parkes receiver group, especially E. Davis, for their help during the setting up of the correlator and the observations. We are also grateful to M. Bailes for comments on the paper and to D. Frail for useful conversations. J. M. W. was supported by NSF Grant AST 92-22435 and a Carleton College Faculty Development Grant.

## REFERENCES

- Ables, J. G., & Manchester, R. N. 1976, *A&A*, 50, 177  
 Alfaro, E. J., Cabrera-Cano, J., & Delgado, A. J. 1992, *ApJ*, 399, 576  
 Alurkar, S. K., Slee, A. B., & Bobra, A. D. 1986, *Australian J. Phys.*, 39, 433  
 Bailes, M., Manchester, R. N., Kesteven, M. J., Norris, R. P., & Reynolds, J. E. 1990a, *Nature*, 343, 240  
 Bailes, M., Manchester, R. N., Kesteven, M. J., Norris, R. P., & Reynolds, J. E. 1990b, *MNRAS*, 247, 322  
 Becker, W., Predehl, P., & Trümper, J. 1992, *IAU Circ.*, No. 5554  
 Bonsignori-Facendi, S. R., Salter, C. J., & Sutton, J. M. 1973, *A&A*, 27, 67  
 Brand, J., & Blitz, L. 1993, *A&A*, 275, 67  
 Brand, J., Blitz, L., & Wouterloot, J. G. A. 1986, *A&AS*, 65, 537  
 Caswell, J. L., Lerche, I. 1979, *MNRAS*, 187, 201  
 Caswell, J. L., Murray, J. D., Roger, R. S., Cole, D. J., & Cooke, D. J. 1975, *A&A*, 45, 239  
 Clifton, T. R., Frail, D. A., Kulkarni, S. R., & Weisberg, J. M. 1988, *ApJ*, 333, 332  
 Cowie, L. L., Hu, E. M., Taylor, W., & York, D. G. 1981, *ApJ*, 250, L25  
 D’Amico, N., Manchester, R. N., Durdin, J. M., Stokes, G. H., Stinebring, D. R., Taylor, J. H., & Brissenden, R. J. V. 1988, *MNRAS*, 234, 437  
 Fich, M., Blitz, L., & Stark, A. A. 1989, *ApJ*, 342, 272  
 Fierro, J. M., et al. 1993, *ApJ*, 413, L27  
 Frail, D. A., Clifton, T. R. 1989, *ApJ*, 336, 854  
 Frail, D. A., Cordes, J. M., Hankins, T. H., & Weisberg, J. M. 1991, *ApJ*, 382, 168  
 Frail, D. A., Goss, W. M., & Whiteoak, J. B. Z. 1994, *ApJ*, 437, 781  
 Frail, D. A., Kulkarni, S. R., & Vashisht, G. 1993, *Nature*, 365, 136  
 Frail, D. A., & Weisberg, J. M. 1990, *AJ*, 100, 743  
 Giovanelli, R., Haynes, M. P. 1988, in *Galactic and Extragalactic Radio Astronomy*, ed. G. L. Verschuur & K. I. Kellermann (New York: Springer), 522 ff  
 Gómez González, J., Guélin, M., Falgarone, E., & Encrenaz, P. 1973, *Astro-phys. Lett.*, 13, 229



- Gordon, K. J., & Gordon, C. P. 1973, *A&A*, 27, 119  
 Goss, W. M., Radhakrishnan, V., Brooks, J. W., & Murray, J. D. 1972, *ApJS*, 24, 123  
 Grabelsky, G. A., Cohen, R. S., Bronfman, L., Thaddeus, P., & May, J. 1987, *ApJ*, 315, 122  
 Graham, J. A. 1970, *AJ*, 75, 703  
 Herbst, W. 1975, *AJ*, 80, 212  
 Humphreys, R. M., & Kerr, F. J. 1974, *ApJ*, 194, 301  
 Johnston, S., Lyne, A. G., Manchester, R. N., Kniffen, D. A., D'Amico, N., Lim, J., & Ashworth, M. 1992, *MNRAS*, 255, 401  
 Kerr, F. J., & Lynden-Bell, D. 1986, *MNRAS*, 221, 1023  
 Kerr, F. J., Bowers, P. F., Jackson, P. D., & Kerr, M. 1986, *A&AS*, 66, 373  
 Kifune, T., et al. 1993, *IAU Circ.*, No. 5905  
 Kulkarni, S. R., & Heiles, C. 1988, in *Galactic and Extragalactic Radio Astronomy*, ed. G. L. Verschuur & K. I. Kellermann (New York: Springer), 95 ff  
 Large, M. I., Vaughan, A. E., & Wielebinski, R. 1968, *Nature*, 220, 753  
 ———. 1969, *Nature*, 223, 1249  
 Lyne, A. G., & Lorimer, D. R. 1994, *Nature*, 369, 127  
 Lyne, A. G., Manchester, R. N., & Taylor, J. H. 1985, *MNRAS*, 213, 613  
 Manchester, R. N., Lyne, A. G., Taylor, J. H., Durdin, J. M., Large, M. I., & Little, A. G. 1978, *MNRAS*, 185, 409  
 Manchester, R. N., Wellington, K. J., & McCulloch, P. M. 1981, in *IAU Symp. 95, Pulsars*, ed. W. Sieber & R. Wielebinski (Dordrecht: Reidel), 445  
 McAdam, W. B., Osborne, J. L., & Parkinson, M. L. 1993, *Nature*, 361, 516  
 Radhakrishnan, V., Goss, W. M., Murray, J. D., & Brooks, J. W. 1972, *ApJS*, 24, 1  
 Shaver, P. A., Radhakrishnan, V., Anantharamaiah, K. R., Retallack, D. S., Wamsteker, W., & Danks, A. C. 1982, *A&A*, 106, 105  
 Srinivasan Sahu, M., & Sahu, K. C. 1993, *A&A*, 280, 231  
 Stacy, J. G., & Jackson, P. D. 1982, *Nature*, 296, 42  
 Strong, A. W., Riley, P. A., Osborne, J. L., & Murray, J. D. 1982, *MNRAS*, 201, 495  
 Taylor, J. H., & Cordes, J. M. 1993, *ApJ*, 411, 674  
 Taylor, J. H., Manchester, R. N., & Lyne, A. G. 1993, *ApJS*, 88, 529  
 Thompson, D. J., et al. 1992, *Nature*, 359, 615  
 van den Bergh, S., & Herbst, W. 1975, *AJ*, 80, 208  
 Vaughan, A. E., Large, M. I., & Wielebinski, R. 1969, *Nature*, 222, 963  
 Weisberg, J., Boriakoff, V., & Rankin, J. 1979, *A&A*, 77, 204  
 Wielebinski, R., Vaughan, A. E., & Large, M. I. 1969, *Nature*, 221, 47